PERGAMON

Journal of Structural Geology 25 (2003) 883–895

JOURNAL OF STRUCTURAL GEOLOGY

www.elsevier.com/locate/jstrugeo

Normal fault growth, displacement localisation and the evolution of normal fault populations: the Hammam Faraun fault block, Suez rift, Egypt

Rob L. Gawthorpe[a,*], Christopher A.-L. Jackson[a], Mike J. Young[a], Ian R. Sharp[b], Adel R. Moustafa[c], Christopher W. Leppard[a]

[a]*Basin and Stratigraphic Studies Group, Department of Earth Sciences, University of Manchester, Manchester M13 9PL, UK*
[b]*Norsk Hydro Research Centre, Sandsliveien 90, Bergen, Norway*
[c]*Department of Geology, Ain Shams University, Cairo 11566, Egypt*

Received 2 September 2001; accepted 25 June 2002

Abstract

Fault segment linkage, migration of the locus of fault activity, and displacement localisation were important processes controlling the late Oligocene–Recent evolution of the normal fault population of the Hammam Faraun fault block, Suez rift. Initial fault activity was distributed across the fault block on fault segments that had attained their final length within 1–2 My of rifting. These initial segments then either grew by increasing displacement and linked to form longer segmented fault zones or died, during a rift initiation phase that lasted 6–8 My. Following this rift initiation phase, displacement became localised onto >25-km-long border fault zones bounding the fault block and many of the early high-displacement intra-block fault zones died. Following displacement localisation onto the major faults bounding the fault block, the locus of maximum displacement continued to migrate, with post-Middle Miocene displacement focused on the western margin of the fault block. This migration of fault activity between major crustal-scale normal faults can be viewed in terms of strain localisation at the rift scale. The results from this study question conventional fault growth models based on final displacement distributions, and highlight the sequential nature of faulting on major normal faults bounding domino-style tilted fault blocks.

Keywords: Normal fault population; Fault growth; Displacement localisation; Suez rift

1. Introduction

The evolution and linkage of fault segments to form continuous, basin-bounding normal fault zones is recognised as a first-order control on the size and shape of sedimentary basins in extensional settings (e.g. Anders and Schlische, 1994; Gawthorpe et al., 1994). The evolution of normal fault zones is therefore recorded in the stratigraphy of rift basins (e.g. Prosser, 1993; Morley, 1999; Contreras et al., 2000; Gawthorpe and Leeder, 2000; Meyer et al., 2002) and in the geomorphology of their hinterlands (e.g. Leeder et al., 1991; Leeder and Jackson, 1993; Eliet and Gawthorpe, 1995; Goldsworthy and Jackson, 2000).

Conventional models of fault growth suggest that faults grow by systematic increases in maximum displacement and length, and that faults within a fault population become linked with time (e.g. Walsh and Watterson, 1988; Cartwright et al., 1995; Dawers and Anders, 1995; Cowie, 1998; Ackermann et al., 2001; Mansfield and Cartwright, 2001). However, the detailed temporal evolution of individual faults and fault populations is still poorly constrained and these aspects of fault growth can only be addressed where information from stratigraphy or landscape allows sequential reconstruction of displacements and lengths of fault zones (Gawthorpe and Leeder, 2000).

Recent studies of ancient fault systems, utilising syn-rift stratigraphy, have begun to provide insights into fault growth histories, but are generally confined to single fault zones. Some of these studies support conventional models of fault growth, where propagation and linkage are important in fault evolution (e.g. Contreras et al., 2000; Dawers and Underhill, 2000). In contrast, others suggest alternative growth models, in which fault lengths are nearly

* Corresponding author.
E-mail address: rob.gawthorpe@man.ac.uk (R.L. Gawthorpe).

0191-8141/03/$ - see front matter © 2002 Elsevier Science Ltd. All rights reserved.
PII: S0191-8141(02)00088-3

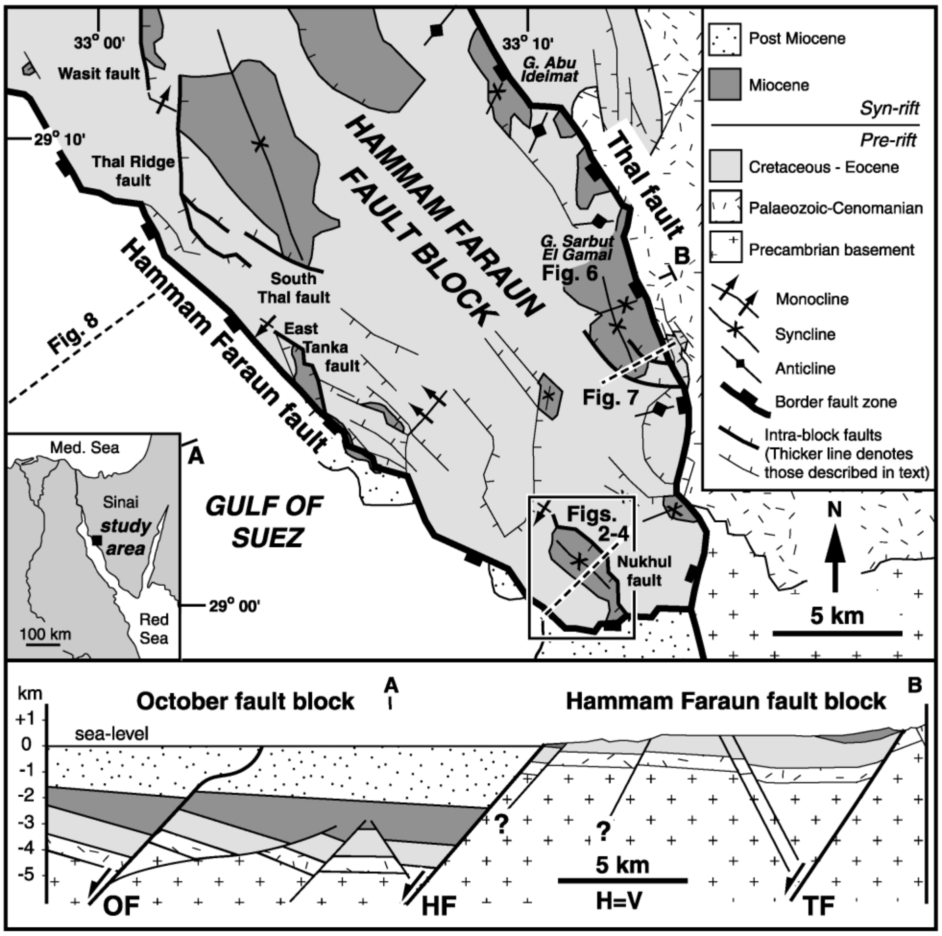

Fig. 1. Simplified geological map and cross-section of the Hammam Faraun fault block highlighting the present day structural geometry of border and intra-block fault zones, and the distribution of Miocene syn-rift sediments (after Moustafa and Abdeen, 1992; Sharp et al., 2000b). Note that the cross-section extends off the SW of the map into the centre of the Gulf of Suez across the October fault block, a major oil field in the Gulf of Suez. TF = Thal fault; HF = Hammam Faraun fault; OF = October fault.

constant from an early stage and faults grow by increasing cumulative displacement (e.g. Meyer et al., 2002). Furthermore, studies from areas of active normal faulting highlight high frequency cyclic activity on major fault zones (e.g. Morley et al., 2000) and switching of activity between major fault zones (e.g. Leeder et al., 1991; Goldsworthy and Jackson, 2000), characteristics that are not readily apparent from studies of ancient fault populations.

In this paper we focus on the temporal evolution of a normal fault population from a 500 km^2 area of the Hammam Faraun fault block, Suez rift (Fig. 1), from rift initiation in the late Oligocene to the present-day. In particular, using a combination of structural and stratigraphic data, we examine how individual fault segments grew, linked and died, and how the fault population evolved during the development of the crustal-scale border faults that bound the Hammam Faraun fault block and intra-block faults within it. The results of the study highlight the sequential nature of faulting with: (i) distributed faulting during the early stages of rifting, (ii) progressive localisation of strain onto major crustal-scale border faults associated with the death of intra-block faults, and (iii) migration of fault activity and localisation of displacement on specific border faults.

2. Methodology

The Hammam Faraun fault block (Fig. 1) is characterised by deeply incised wadis and lack of vegetation that provide pseudo-3D exposure of fault zones and stratigraphy. This allows structural and stratigraphic features to be walked out both parallel to, and across, the main fault zones, enabling plan-form and cross-sectional geometries to be quantified. Previous work has documented structural style of the main fault zones and the thickness of pre-rift formations allowing present-day displacement variations along the fault zones to be determined (e.g. Moustafa and Abdeen, 1992). Our work has focused on mapping the geometry of fault zones, associated folds, and syn-rift stratigraphic units using high-resolution aerial photographs, SPOT images and photopanoramas. In addition, we have interpreted pre-stack depth migrated 3D seismic data

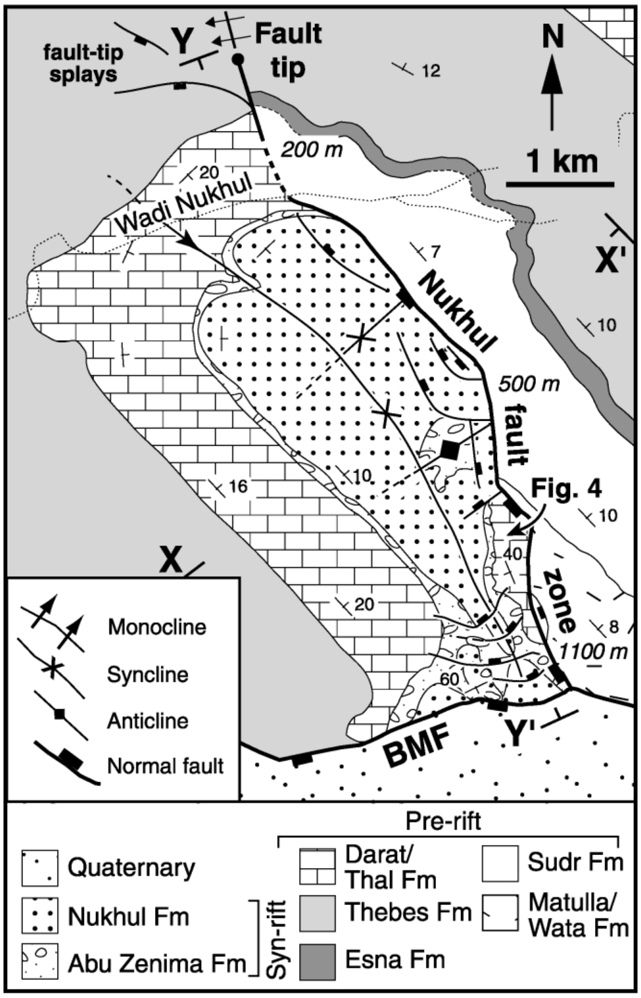

Fig. 2. Simplified geological map of the intra-block, Nukhul fault zone (see Fig. 1 for location). Values in metres shown along the fault indicate displacement. Note the transverse folds that die out away from the fault zone over a distance of ca. 1 km, and the fault tip splays and monocline at the northern termination of the fault zone. The upper part of the Abu Zenima Formation and the lower part of the Nukhul Formation form cliffs that impact on map patterns (see topographic profiles in Fig. 3). BMF = Baba–Markha Fault; X–X′ and Y–Y′ indicate cross-sections illustrated in Fig. 3.

from the hanging wall of the Hammam Faraun fault zone. We have paid particular attention to thickness variations, facies distributions and onlap/truncation patterns within the syn-rift stratigraphy in order to reconstruct the location of fault tips, fault segment lengths, fault/fold geometry and locus of fault activity for different times in the rift history (cf. Gawthorpe et al., 1997; Gupta et al., 1999; Sharp et al., 2000b; Jackson et al., 2002). Stratigraphic ages are based on biostratigraphic (Krebs et al., 1997) and magnetostratigraphic (Bentham et al., 1995) studies. In addition, dating of key stratal surfaces has been established using marine Sr-isotope stratigraphy following the approach of McArthur et al. (2001) to convert $^{87}Sr/^{86}Sr$ ratios of oysters to numerical ages.

3. The Hammam Faraun fault block

The Suez rift is the NW extension of the Red Sea rift and developed in the Oligo-Miocene due to the separation of the Arabian plate from Africa. The Hammam Faraun fault block is exposed on the Sinai peninsula and is one of the main fault blocks in the central dip province of the Suez rift (e.g. Patton et al., 1994; Fig. 1).

The fault block has a half-graben geometry, dipping moderately to the east (12–15°), is up to 25 km wide and is bounded to the east and west by major normal fault zones, the Thal and Hammam Faraun fault zones, respectively (Moustafa and Abdeen, 1992; Moustafa, 1996; Sharp et al., 2000a; Fig. 1). These major border fault zones are in excess of 25 km long, dip steeply to the west (60–80°) and have displacements up to 5 km. In plan view the border faults have a zigzag pattern; the dominant fault strike is NW–SE, with subordinate N–S-, NNE–SSW- and E–W-trending segments. The southern boundary of the fault block is marked by the prominent E–W-trending Baba–Markha fault. Internally the fault block is dissected by a series of mesoscale synthetic and antithetic fault zones (here termed intra-block fault zones) that have displacements of <1 km, and have a similar orientation and zigzag pattern to the border faults (Fig. 1).

Folding is an important deformation mechanism adjacent to the fault zones, with fold axes orientated both parallel and perpendicular to the fault zones. Fault-parallel anticlines and synclines occur within the footwall and hanging wall, respectively, and can be traced laterally, parallel to fault strike, into unbreached monoclines located at the fault tips (e.g. Tanka and Nukhul fault zones; Fig. 1; Sharp et al., 2000a; Jackson et al., 2002). Fault-perpendicular folds are also pronounced in the immediate hanging wall of fault zones and die out within several hundred metres to 1–2 km of the fault zones. Stratigraphic relationships around these folds provide important information on the style of surface deformation around the fault zones and the timing of linkage of adjacent fault segments.

Exposed pre-rift strata in the Hammam Faraun fault block mainly comprise carbonates and subordinate mudstones of late Cretaceous to Eocene age (Sudr, Thebes, Darat, Thal and Tanka Formations) and are interpreted to have been sub-horizontal prior to extension (e.g. Moustafa and Abdeen, 1992; Moustafa, 1996; Sharp et al., 2000b). Regional studies by Moustafa have also mapped older Mesozoic and Palaeozoic pre-rift formations exposed in the footwall of the Thal fault zone and locally exposed along the eastern side of the fault block (e.g. Moustafa and Abdeen, 1992; Moustafa, 1996). These older pre-rift formations overlie Precambrian ‘Pan-African’ basement and comprise Cambrian to Lower Cretaceous Nubian sandstones and a Cretaceous mixed carbonate clastic succession (Raha, Wata and Matulla Formations).

The pre-rift is unconformably overlain by a clastic syn-rift succession of Oligo-Miocene non-marine (Abu Zenima

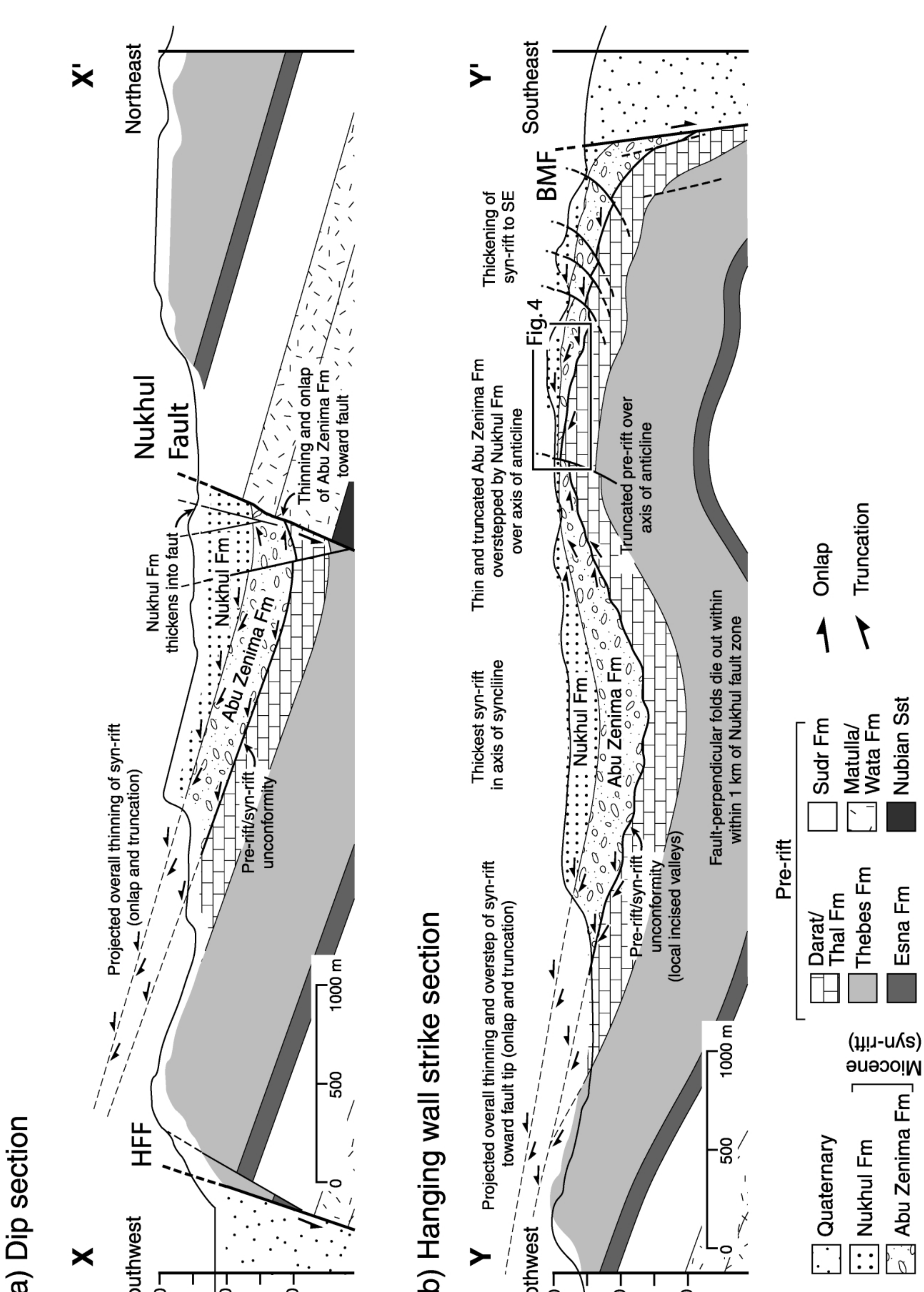
a) Dip section
X
X'
Southwest
Northeast
HFF
Nukhul
Fault
Projected overall thinning of syn-rift
(onlap and truncation)
Nukhul Fm
thickens into faut
Nukhul Fm
Abu Zenima Fm
Pre-rift/syn-rift
unconformity
Thinning and onlap
of Abu Zenima Fm
toward fault
200
0
-200
Elevation (m)
0
500
1000 m
b) Hanging wall strike section
Y
Y'
Nothwest
Southeast
Projected overall thinning and overstep of syn-rift
toward fault tip (onlap and truncation)
Thickest syn-rift
in axis of syncliine
Thin and truncated Abu Zenima Fm
overstepped by Nukhul Fm
over axis of anticline
Thickening of
syn-rift to SE
Fig. 4
BMF
Nukhul Fm
Abu Zenima Fm
Pre-rift/syn-rift
unconformity
(local incised valleys)
Truncated pre-rift over
axis of anticline
Fault-perpendicular folds die out within
within 1 km of Nukhul fault zone
200
0
-200
Elevation (m)
0
500
1000 m
Quaternary
Nukhul Fm
Abu Zenima Fm
Miocene
(syn-rift)
Pre-rift
Darat/
Thal Fm
Thebes Fm
Esna Fm
Sudr Fm
Matulla/
Wata Fm
Nubian Sst
Onlap
Truncation

Formation; 24–21.5 Ma), tidal to marginal marine (Nukhul Formation; 21.5–19.7 Ma) and open marine (Rudeis Formation; 19.7–15.5 Ma) strata (ages based on Patton et al., 1994; Krebs et al., 1997). The Abu Zenima and Nukhul Formations are interpreted to have been deposited during a slow subsidence rift-initiation phase, whereas the Rudeis Formation is interpreted to have been deposited during a high subsidence rift-climax phase (e.g. Garfunkel and Bartov, 1977; Richardson and Arthur 1988; Steckler et al., 1988; Patton et al., 1994; Krebs et al., 1997). The Kareem Formation (15.5–14 Ma) is the youngest formation exposed in the study area, but in the hanging wall of the Hammam Faraun fault zone, several kilometres of younger strata (e.g. Belayim, South Gharib, Zeit, Wardan formations) are preserved beneath the Gulf of Suez (e.g. Patton et al., 1994; Fig. 1).

4. Evolution of the intra-block fault zones

The importance of fault segment growth and linkage in the evolution of the intra-block fault zones is well illustrated by the Nukhul fault zone and associated early syn-rift stratigraphy (Figs. 2 and 3). The Nukhul fault zone has a characteristic zigzag pattern, comprising NW–SE- and N–S-trending segments in map view. Based on the offset of pre-rift formations of known thickness, the fault zone overall loses displacement from a maximum in the south (ca. 1000 m) to a well defined tip point and associated fault-tip monocline in the north (Fig. 2; Moustafa and Abdeen, 1992). The southern end of the fault zone terminates abruptly against the Baba–Markha fault.

The Nukhul fault dips steeply (60–80°) to the SW and has a prominent fault-parallel syncline developed along its length (Figs. 2 and 3a). Pre-rift and early syn-rift strata in the immediate hanging wall of the NW–SE-trending fault segments dip away from the fault zone (20–45° to the SW) whereas, in the footwall, pre-rift strata dip gently ($<10°$) to the NE, giving an overall faulted monocline geometry. The syn-rift succession in the immediate hanging wall of the fault zone displays a progressive decrease in dip from 40° at the base of the Abu Zenima Formation, to sub-horizontal within the youngest exposed Nukhul Formation.

The Abu Zenima Formation is thickest (up to 150 m) along the axis of the fault-parallel hanging wall syncline and onlaps and thins towards the fault zone, the thinning partially achieved by intraformational angular unconformities that are most pronounced adjacent to the fault zone (Fig. 3a). Projection of bedding within the Abu Zenima Formation also suggests thinning to the southwest of the fault-parallel syncline, up the hanging wall dipslope (Fig. 3a). In contrast, individual stratal units within the Nukhul Formation thicken into the fault zone.

The Abu Zenima and Nukhul formations also show major fault-parallel variations in thickness and facies (Fig. 3b). The Abu Zenima Formation has two distinct depocentres, each ca. 3 km long, that parallel the NW–SE-trending segments (Figs. 2 and 3b). These two depocentres are separated from one another by an area of thin syn-rift that is associated with a fault-perpendicular anticline located in the hanging wall of the N–S-trending fault segment (Figs. 2, 3b and 4). The fault-perpendicular folds affect both pre- and earliest syn-rift strata and die out away from the Nukhul fault zone over a distance of ca. 1 km (Figs. 2 and 3b). Although the upper and lower boundaries of the Abu Zenima Formation are erosional, mapping of distinctive internal stratal units indicates progressive thinning, onlap and intraformational truncation onto the fault-perpendicular anticline in a manner that mimics the overall thickness variations of the formation (Figs. 3b and 4). Projection of bedding dips and thickness variations also suggests thinning of the Abu Zenima Formation and erosion and overstep of pre-rift stratigraphy towards the northern tip of the Nukhul fault zone (Fig. 3b).

Thickness variations within the lower part of the Nukhul Formation are similar to those in the Abu Zenima Formation, but most of the stratal units within the upper part of the Nukhul Formation do not thin over the fault-perpendicular anticline (Fig. 4). Instead, the Nukhul Formation progressively thickens, and facies become more distal, to the south, up to where the Nukhul fault zone and associated syn-rift stratigraphy are truncated by the E–W-trending Baba–Markha fault. Thus there appears to have been a single Nukhul depocentre, at least as long as the present-day trace of the Nukhul fault zone (>7 km) and probably longer, prior to truncation by the Baba–Markha fault zone.

The stratigraphic data presented here suggest that the present-day geometry of the Nukhul fault zone formed by growth and linkage of two, initially isolated ca. 3-km-long fault segments, the lengths of which became established during the earliest stages of rifting. Onlap and thickness relationships suggest that, during Abu Zenima times, deposition occurred in fault-parallel growth synclines in

Fig. 3. (a) Dip section across the Nukhul fault zone. Note the onlap and thinning of the Abu Zenima Formation towards the fault zone and the projected thinning up the hanging wall dip slope. Bedding within the upper part of Nukhul Formation is sub-horizontal and stratal units expand into the fault. HFF = Hammam Faraun fault zone. (b) Strike section in the immediate hanging wall of the Nukhul fault zone highlighting the fault-perpendicular folding of pre- and syn-rift strata. The Abu Zenima Formation is thickest in the fault-perpendicular syncline and in the immediate footwall of the Baba–Markha fault (BMF) and thins and onlaps onto the fault-perpendicular anticline. Also note the projected thinning and overstep of the syn-rift to the northwest. See Fig. 2 for location of the cross-sections and note vertical exaggeration of the sections.

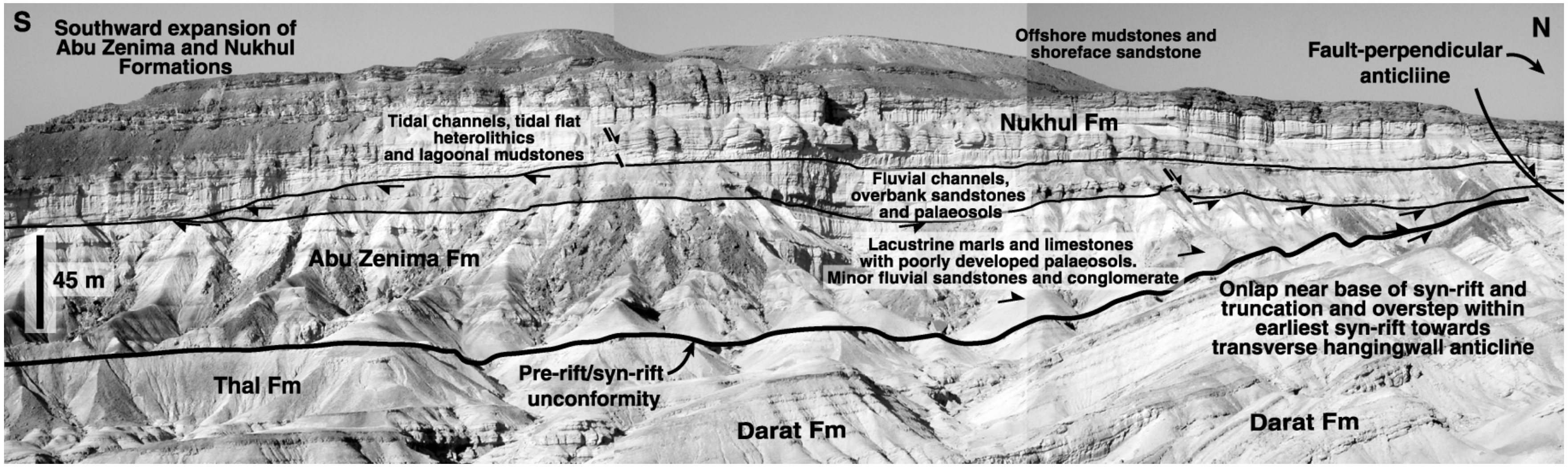

Fig. 4. Photopanorama of strike section, looking W, into the immediate hanging wall of the southern NW–SE-trending segment of the Nukhul fault zone to the south of the fault-perpendicular anticline. Note intraformational thinning, onlap and truncation within the early syn-rift Abu Zenima Formation towards the N (i.e. towards the fault-perpendicular anticline), whereas the upper part of the Nukhul Formation is relatively sheet-like. See Figs. 2 and 3 for location.

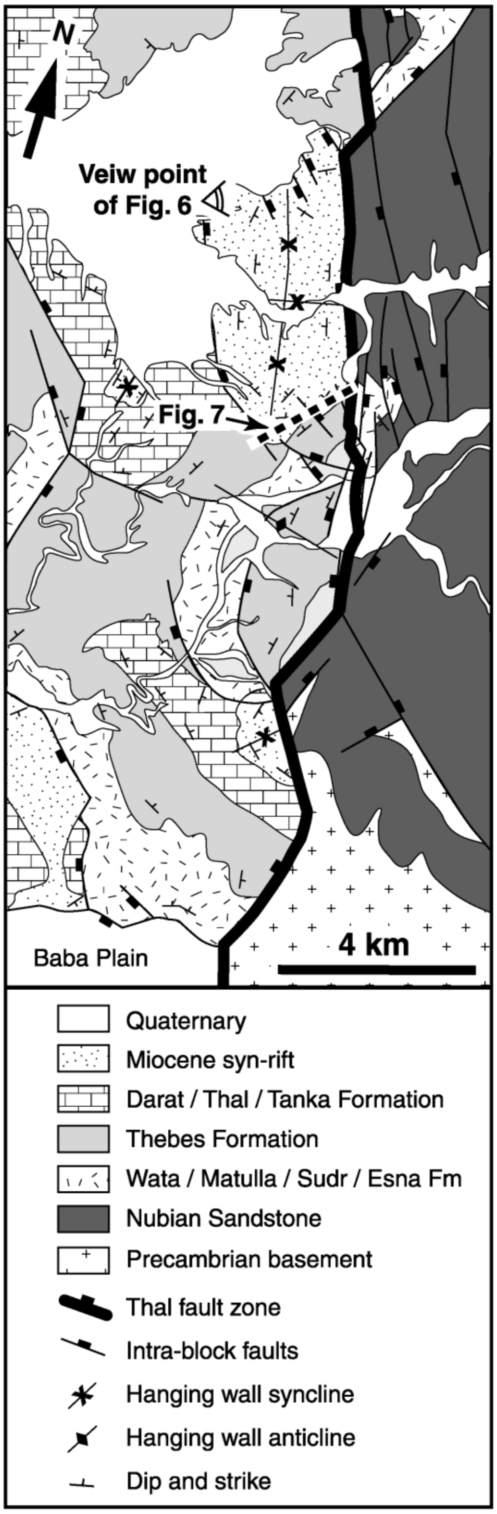

Fig. 5. Simplified geological map of the central and southern part of the Thal fault zone illustrating the zigzag pattern of the border fault and the relationship between Miocene syn-rift depocentres and NW–SE-trending fault segments. Note the fault-parallel and fault-perpendicular folding in the hanging wall of the fault zone and 'scoop-shape' of the syn-rift depocentres (modified after Moustafa and Abdeen, 1992; Young et al., 2002).

the hanging walls of the two NW–SE-trending fault segments. The dip of the Abu Zenima Formation away from the fault segments and the thinning and local unconformities in the immediate hanging wall of the fault segments suggest that the fault segments were blind and represented at surface by fault-propagation monoclines (cf. Gawthorpe et al., 1997; Hardy and McClay, 1999). This is supported by the presence of an unbroken fault-tip monocline at the northern end of the Nukhul fault zone (Fig. 2). The along-strike variations in thickness suggest that the two depocentres were separated by an area of low hanging wall subsidence, the fault-perpendicular anticline (cf. Anders and Schlische, 1994), located in the hanging wall of the N–S-trending fault jog. The thinning over this anticline and back towards the fault zone suggests that this present-day N–S-trending fault jog was probably an unbreached relay ramp during Abu Zenima times.

In contrast, in the Nukhul Formation, thickening into the fault zone and the continuity of stratal units over the fault-perpendicular anticline suggest that the fault segments were surface breaking faults, and that the relay ramp had become breached. Thus, during deposition of the Nukhul Formation, the fault zone behaved as a single, hard-linked, segmented fault zone with displacement progressively increasing to the south. The cross-cutting relationships between the Nukhul fault zone and the Baba–Markha fault indicate that the latter is a younger structure truncating the southern end of the Nukhul fault zone.

Along-strike variations in thickness and facies of the Abu Zenima and Nukhul formations are characteristic features of many of the intra-block fault zones within the Hammam Faraun fault block (Fig. 1). The East Tanka fault zone (Jackson et al., 2002; Fig. 1) evolved in a similar way to the Nukhul fault zone, with two distinct Abu Zenima depocentres in the hanging wall of NW–SE-trending fault segments, separated by a hanging wall fault-perpendicular anticline. The fault zone is interpreted to have evolved from two isolated, but interacting segments during Abu Zenima times, to a hard-linked fault zone bounding a single Nukhul depocentre (Jackson et al., 2002). In the northwest of the Hammam Faraun fault block, a faulted monocline between the Thal Ridge and Wasit faults (Fig. 1), which is onlapped by the Nukhul Formation, is also interpreted to represent a breached Nukhul-aged relay ramp (Moustafa and Abdeen 1992; Sharp et al., 2000b).

The syn-rift stratigraphy in the hanging walls of the Nukhul, East Tanka, Thal Ridge and Wasit fault zones suggests that fault growth and linkage was ongoing during deposition of the Abu Zenima and Nukhul formations. However, some early faults also became inactive during Abu Zenima and Nukhul times. For example, the South Thal fault (Fig. 1) has approximately 40 m of displacement at the pre-rift/syn-rift unconformity, whereas the upper part of the Nukhul Formation extends as a continuous, unfaulted sheet from the hanging wall to the footwall (Sharp et al., 2000b; their figs. 8 and 9).

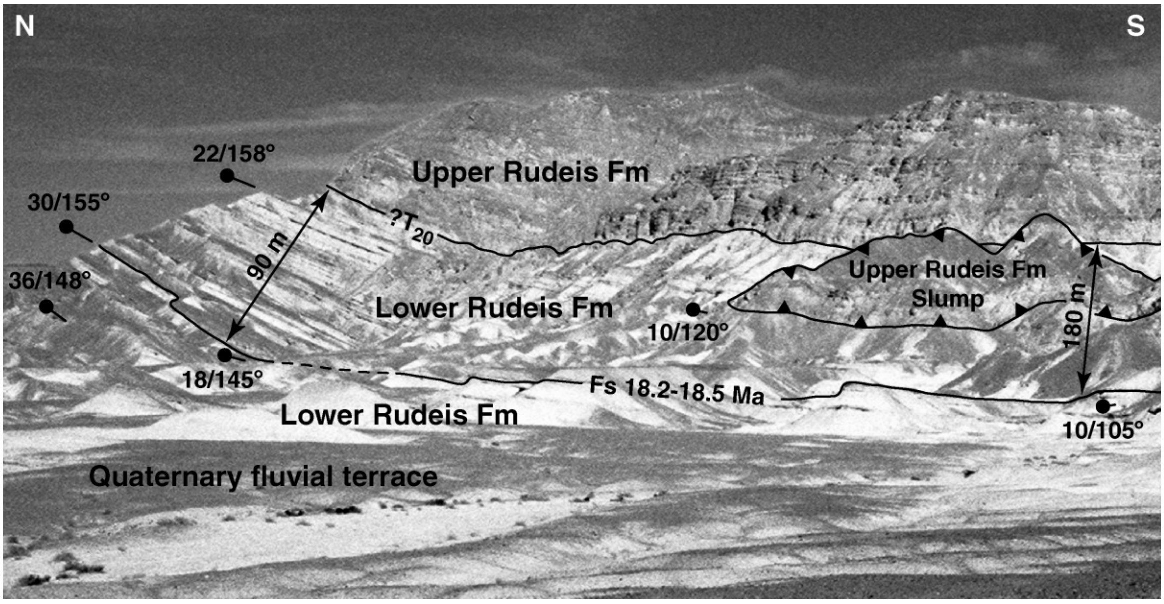

Fig. 6. Photopanorama, looking E/NE towards the footwall, of the immediate hanging wall syn-rift stratigraphy at the northern end of the G. Sarbut El Gamal segment (see Fig. 5 for location). Fault segment centre is on the right (S) and the hanging wall high that forms the northern end of the fault segment is on the left (N). Measurements, based on logged sections, indicate the thinning of the syn-rift towards the hanging wall high at northern end of the NW–SE-trending G. Sarbut El Gamal segment (stratal unit is foreshortened at right-hand side due to it being largely exposed in low-ground in front of cliff). Also note change in dip and strike of the syn-rift towards the segment boundary and the progressive decrease in dip up stratigraphy. The major flooding surface within the Lower Rudeis Formation (Fs) is the same as the datum in Fig. 7; T_{20} is the position of the graphic correlation terrace of Krebs et al. (1997).

5. Evolution of the border fault zones

The eastern border fault zone (Thal fault zone) of the Hammam Faraun fault block displays a similar structural geometry to the intra-block Nukhul fault zone (Fig. 1). Based on known pre-rift formation thicknesses and mapping of the pre-rift exposed in the footwall and hanging wall of the fault zone, vertical offset across the fault can be estimated with an error of <150 m. Displacement is greatest in the south (ca. 2 km) where the Thal and Baba–Markha faults branch, and decreases northward to 1.3 km at Gebel Sarbut El Gamal, 600–700 m at Gebel Abu Ideimat, and ultimately to zero at the fault tip over 30 km to the north of the branch point (Moustafa and Abdeen 1992; Young et al., 2002; Fig. 1). The northward decrease in displacement is accompanied by the progressive northward younging of pre-rift strata exposed in the footwall of the fault zone, suggesting decreasing footwall uplift to the north.

The northward decrease in displacement is not smooth, but shows considerable variation (Young et al., 2002). Displacement highs, where displacement is generally >1 km, are associated with the NW–SE-trending segments (termed fault strands by Sharp et al., 2000a) that contain areas of thick syn-rift stratigraphy in their hanging walls (e.g. G. Sarbut El Gamal; Figs. 1 and 5). In all, there are four main NW–SE-trending segments along the length of the Thal fault zone that are 3–8 km long and have doubly-plunging fault-parallel synclines in their hanging walls that give the hanging wall a scoop-shaped geometry (Fig. 5).

The NW–SE-trending fault segments are now linked by shorter NNE–SSW- and E–W-trending segments that are areas of relative low displacement (generally <300–500 m), with hanging wall highs that are presently devoid of syn-rift stratigraphy (Figs. 1 and 5). The structure of the hanging wall highs is either monoclinal, dipping into the hanging wall, or a fault-perpendicular anticline. Fault splays extend from the branch points between the different segments (Fig. 5).

Mapping of syn-rift stratal units around the hanging wall depocentres and onto the margins of the fault-perpendicular anticlines shows that the thickest syn-rift is located in the centre of the NW–SE-trending fault segments and that the syn-rift thins, along strike, towards the fault-perpendicular anticlines. These relationships are well displayed by the G. Sarbut El Gamal segment where stratal units near the top of the Lower Rudeis Formation thin over a distance of ca. 3.5 km from 190 m near the centre of the fault segment to <90 m near to the northern segment boundary (Fig. 6). This thinning is also associated with a marked change in dip and strike of the beds as they are traced onto the margins of the fault-perpendicular anticline (Figs. 5 and 6). As in the syn-rift stratigraphy of the hanging wall of the Nukhul fault zone, dips within the syn-rift progressively shallow up section (Fig. 6).

Although the present-day structural geometry of the Thal fault zone is similar to the Nukhul and other intra-block fault zones, the timing of fault growth and linkage along the Thal border fault zone is significantly different. These differences in evolution are clearly represented in the stratigraphy of the G. Sarbut El Gamal segment (Figs. 1, 5

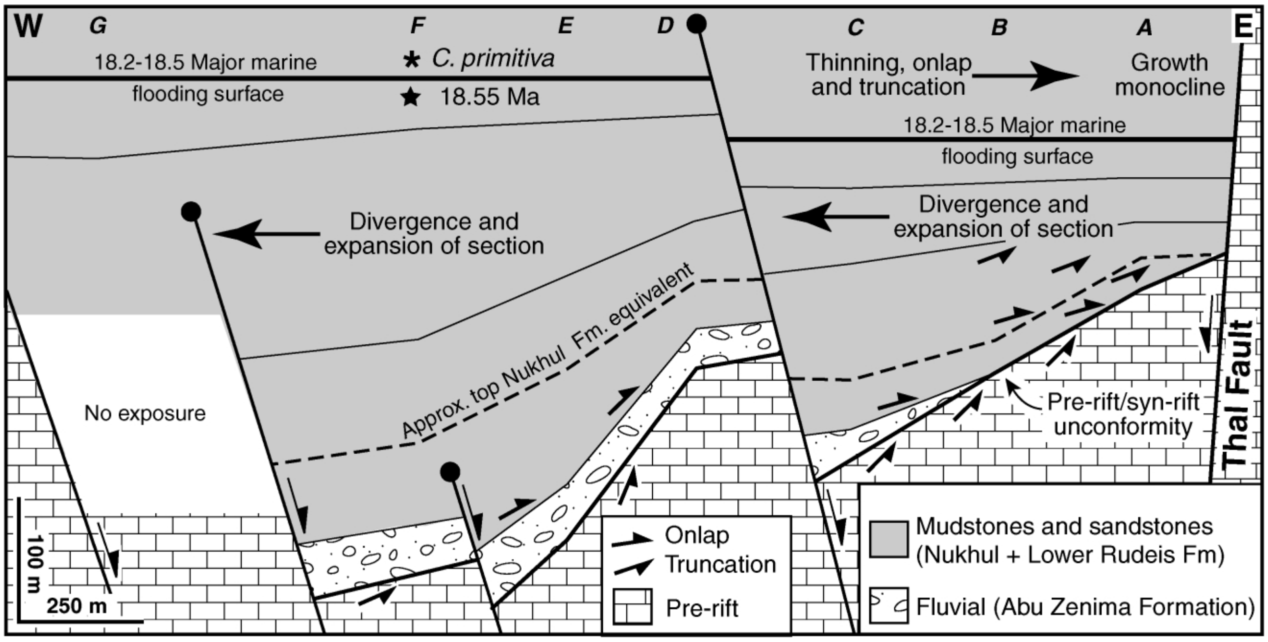

Fig. 7. Dip correlation panel in the immediate hanging wall of the Thal fault at the southern end of the G. Sarbut El Gamal segment. The correlation based on mapping key stratal surfaces and graphic logging, and is partially hung on the 18.2–18.5 Ma marine flooding surface shown in Fig. 6 (see Fig. 5 for location). Note the major thickening of the early syn-rift into the hanging walls of antithetic faults and the death of these faults within the Lower Rudeis Formation. Letters A–G show the positions of measured sections.

and 6). A number of dated stratal surfaces can be mapped around the syn-rift depocentre, allowing constraints to be placed on the timing and style of deformation along this segment of the fault zone. The lower part of the syn-rift succession is dominated by offshore mudstones and sandstones, with locally developed fluvial Abu Zenima Formation, and is capped by a major marine flooding surface, above which the succession is dominated by mudstones (Figs. 6 and 7). The presence of the benthic foraminifera *Cancris primitiva* (D. Pivnik, pers. comm., 2001) and ages based on Sr-isotope ratios of oysters and the marine Sr isotope curve (McArthur et al., 2001) suggest that the major flooding surface capping the lower syn-rift succession is 18.5–18.2 Ma (Lower Rudeis Formation). In the south of the G. Sarbut El Gamal segment, the early syn-rift succession shows a pronounced westward increase in thickness, from ca. 100 m against the Thal Fault to ca. 400 m, 2.5 km to the west (Fig. 7). These thickness changes are linked to a series of antithetic faults, several of which are overstepped before the major marine flooding surface that caps this early syn-rift succession. These data suggest that antithetic faults were the main surface-breaking faults controlling early syn-rift deposition and that they became inactive during Lower Rudeis Formation times. In contrast, thinning, onlap and truncation of strata towards the Thal fault zone and the dip of the syn-rift away from the fault suggest it was blind, and its surface expression was that of a west-facing fault propagation monocline during deposition of the Lower Rudeis Formation (cf. Gawthorpe et al., 1997; Sharp et al., 2000a) (Fig. 7).

Thickness data from stratal units above the Lower Rudeis major flooding surface show pronounced along-strike

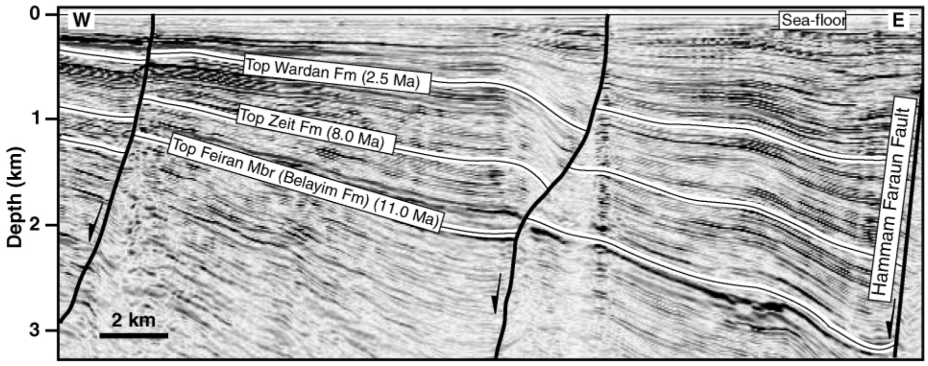

Fig. 8. Pre-stack depth migrated seismic section in the hanging wall of the Hammam Faraun fault showing interpretation of the late Miocene–Recent stratigraphy (see Fig. 1 for location). Note marked thickening into the fault within the post-Feiran Member (Belayim Formation) section suggesting major activity on the fault zone. Uplifted Quaternary marine terraces in the footwall suggest the fault has been active in late Quaternary times.

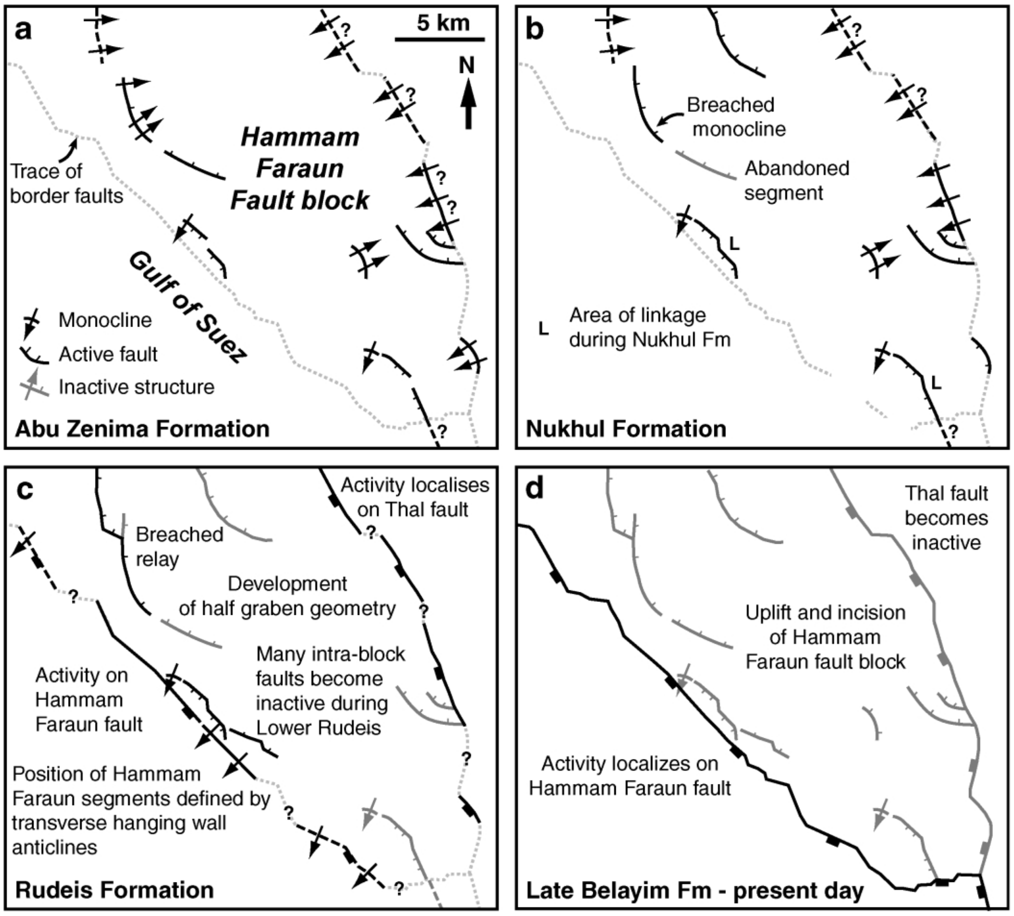

Fig. 9. Evolution of the Hammam Faraun fault population. (a) Abu Zenima Formation (late Oligocene–earliest Miocene). (b) Nukhul times (Lower Miocene). (c) Rudeis times (Lower Miocene–early Middle Miocene). (d) post late Belayim Formation (Middle Miocene–Recent). See text for discussion.

thinning from the centre of the G. Sarbut El Gamal segment onto the hanging wall highs associated with the NNE–SSW-trending fault jogs (Figs. 5 and 6). These stratigraphic relationships, together with the general distribution of syn-rift along the Thal fault zone, indicate that displacement lows associated with the NNE–SSW- and E–W-trending segments were a prominent feature in the hanging wall of the Thal fault zone until at least late Rudeis Formation times (ca. 16.5 Ma). Thus during the early stages of rifting, the Thal fault zone was probably composed of 4–8 km long, isolated fault segments and did not become a major, hard-linked border fault zone until late Rudeis Formation times, some 6–7 Ma after the start of rifting. The present-day expression of the hanging wall highs and the lack of late syn-rift stratigraphy preserved over them suggest that these areas of displacement deficit along the Thal fault zone were not eliminated following linkage.

A relatively late age is also suggested for the main phase of movement on the Hammam Faraun fault zone that forms the western margin of the Hammam Faraun fault block (Figs. 1 and 8). Seismic data suggest that this is a major fault zone with ca. 5 km displacement of the pre-rift/syn-rift unconformity (Moustafa and El Shaarawy, 1987). However, mapping of the late Middle Miocene to Recent section illustrates clear expansion towards the fault zone and ca. 3 km of post late Middle Miocene hanging wall subsidence (Fig. 8). Furthermore, late Quaternary coral terraces in the Wadi Tanka area at elevations of ca. 10–15 m above present sea-level suggest recent uplift in the footwall of the Hammam Faraun fault zone. These data indicate the Hammam Faraun fault accrued most of its displacement late in the evolution of the Suez rift and is still active.

6. Evolution of the Hammam Faraun fault population

Analysis of intra-block and border fault zones and adjacent syn-rift stratigraphy from the Hammam Faraun area of the Suez rift indicates the importance of fault segment interaction and linkage, and migration of the site of maximum fault activity in the evolution of normal fault populations. The study also highlights the importance of fault-related folding (both fault propagation folds above blind normal faults, and fault-perpendicular folds associated with along strike variations in displacement) in controlling the structural style around segmented normal fault zones.

In the Hammam Faraun fault block, initial fault activity was distributed across the fault block on short, typically

< 4 km long, low displacement (several hundred metres) fault segments that were isolated or interacted with their neighbours (Fig. 9a). The presence of the Abu Zenima Formation at the present-day tips of these fault segments suggests that the faults attained their final lengths very early in their growth. Interaction between segments occurred throughout Abu Zenima to Lower Rudeis times (24–18 Ma) with the locus of fault activity migrating as some fault zones grew by segment linkage whilst others died (Fig. 9a and b). During this rift initiation phase, many of the intra-block fault zones (e.g. Nukhul fault zone) were surface-breaking and had greater displacement than the fault segments that became the Thal border fault zone (Fig. 9b).

Restriction of footwall-derived fan deltas and turbidites to the immediate hanging wall of the Thal fault zone, where the Rudeis Formation is thickest, suggests that the Thal fault zone began to develop into a major surface-breaking fault zone during Rudeis times (e.g. Garfunkel and Bartov, 1977; Patton et al., 1994; Sharp et al., 2000a,b; Young et al., 2002; Fig. 9c). Up to 2 km of early to late Miocene stratigraphy in the hanging wall of the Hammam Faraun fault zone suggest that, like the Thal fault zone, it had also become a major border fault zone by late Rudeis times (Fig. 9c). Localisation of displacement onto the major fault zones bounding the Hammam Faraun fault block was progressive, occurring some 6–7 My after the onset of rifting and was associated with the death of many of the intra- block faults (Fig. 9c). These intra-block fault zones were subsequently rotated about a horizontal axis by tilting of the Hammam Faraun fault block due to continued movement on the Thal and/or Hammam Faraun fault zones (Sharp et al., 2000b).

The locus of fault activity continued to migrate following localisation of displacement onto the border fault zones. The thick late Miocene–Recent stratigraphy in the hanging wall of the Hammam Faraun fault zone, together with the fact that the Hammam Faraun fault block is now uplifted and incised, indicate that displacement became localised on the Hammam Faraun fault zone, and that the Thal fault died (Fig. 9d).

7. Implications for fault growth and fault population evolution

7.1. Fault growth models

The presence of the earliest syn-rift Abu Zenima Formation close to the present-day tips of many of the intra-block and border fault segment suggest the segments attained their final trace length very early, within the first ca. 2.5 My of rifting. Thus, during the initial stages of rifting, fault growth was characterised by rapid lateral propagation, and thereafter, fault segments grew by accumulation of displacement with minimal lateral propagation. These observations suggest that fault growth did not follow conventional fault growth models, where faults grow by systematic increase in both displacement and length with time (e.g. Walsh and Watterson, 1988; Cartwright et al., 1995; Dawers and Anders, 1995). These models are largely based on final maximum displacement–fault length scaling relationships where the temporal evolution is largely inferred from the final structure. Other recent studies, also utilising syn-rift stratigraphy to constrain the temporal growth of normal faults, from the Timor Sea (Meyer et al., 2002) and East African rift (Morley, 1999), identify similar fault growth histories to those presented here from the Suez rift. However, there are few studies focusing on the early syn-rift stratigraphy of rift basins that would allow the initial fault geometry to be established. Thus, at present, it is difficult to confirm if this conclusion is a general feature of the early stages of fault growth or not.

Another characteristic feature of fault growth models based on final displacement–length relationships is that a segmented fault zone formed by linkage of adjacent segments behaves in a self-similar manner in comparison with isolated fault segments (e.g. Cartwright et al., 1995; Dawers and Anders, 1995). A corollary of this model is that a recently linked fault zone that is under-displaced with respect to its new length will re-equilibrate, bringing the new lengthened fault zone to an appropriate displacement–length scaling relationship by migration of the locus of maximum displacement to the site of linkage (e.g. Cartwright et al., 1995). In the Hammam Faraun fault block the sites of segment linkage along both the intra-block and border fault zones are still prominent structural highs, for example the fault-perpendicular anticline in the hanging wall of the Nukhul fault zone (Figs. 2–4) and the segment boundaries along the Thal fault zone (Figs. 1, 5 and 6). Thus displacement deficits at sites of linkage seem to be largely maintained along the fault zones where the stratigraphy indicates that they formed by linkage of initially separate segments.

7.2. Fault population evolution

The dynamics of fault population evolution illustrated in this paper have important implications for the tectono-stratigraphic evolution of rifts. The Hammam Faraun fault population evolved from an initial stage where deformation was distributed across the fault block on several isolated to weakly interacting fault segments, through a stage of fault segment linkage, to a situation where deformation was localised on major border faults. The localisation of displacement onto the crustal-scale border faults bounding the Hammam Faraun fault block was associated with a reduction in the number of active faults due to the death of many of the intra-block faults (cf. Fig. 9b and c). Strain localisation and reduction in the number of small faults in a fault population as described here is similar to observations on small to moderate sized faults with displacements < 200 m in the Timor sea (Meyer et al., 2002) and the results of numerical (e.g. Cowie, 1998; Cowie et al., 2000) and analogue models (e.g. Ackermann et al., 2001; Mansfield and Cartwright, 2001). A notable difference between the evolution of the Hammam Faraun fault population and the Timor Sea population described by Meyer et al. (2002) is that the border faults bounding the Hammam Faraun fault block were not major surface-breaking normal faults during the rift initiation stage. Several synthetic and antithetic intra-block fault zones, such as the Nukhul fault zone, had the highest displacements during deposition of the Abu Zenima and Nukhul Formations, but died during, or soon after, localisation of displacement onto the Thal fault zone during Rudeis times. This contradicts previous suggestions that a hierarchy of fault sizes is established very early in the evolution of a fault population and that the largest faults always had the highest displacement rates (e.g. Nicol et al., 1997; Meyer et al., 2002).

Even after displacement became localised on the Thal border fault zone, the fault population continued to evolve, with migration of maximum fault activity from the Thal fault zone onto the Hammam Faraun fault zone (cf. Fig. 9c and d). This highlights the role of sequential fault activity, rather than simultaneous activity on the border fault zones, in developing domino-style tilted fault blocks. The basinward migration of fault activity from the Thal fault zone to the Hammam Faraun fault zone is similar to the hanging wall migration of faulting on major normal faults in areas of active normal faulting such as central Greece (e.g. Roberts and Jackson, 1991; Gawthorpe et al., 1994; Goldsworthy and Jackson, 2000) and may be a general feature of extensional systems.

Migration of fault activity between the border fault zones may reflect a similar strain localisation process to that which operated on the scale of Hammam Faraun fault block, but on a rift scale. Thus, on a rift scale, deformation on major normal faults becomes increasingly localised onto larger, more linked fault systems. In the central dip province of the Suez rift, this rift-scale localisation process led to the focusing of fault activity on the >80-km-long Coastal Fault Belt (Garfunkel and Bartov, 1977), which comprises the Hammam Faraun fault zone in the north and, further south, the Baba–Markha, Nezzazat, Ekma, Abu Durba and Araba faults. In order to establish if localisation of fault activity at a rift scale is a general feature of continental extensional tectonics, studies of the long-term (10^5–10^7 years) evolution of major normal fault zone arrays from individual rift provinces are required. Integration of oil industry 3D seismic surveys to give basin-wide coverage across several crustal-scale fault blocks may represent the best approach to investigating the evolution of fault populations at the rift scale.

Acknowledgements

This research is supported by BP, Norsk Hydro and the Natural Environment Research Council (Research Grant GR3/12947 to Gawthorpe, and Studentships GT04/98/197/ES to Jackson, GT04/97/196/ES to Young and NER/S/J/2000/04064 to Leppard). We thank Gulf of Suez Petroleum Company and BP for permission to publish Fig. 5 and for providing logistical help in the field. This research developed from initial work in collaboration with John Underhill, Sanjeev Gupta and Ian Carr on the El Qaa fault block. Dave Pivnik is thanked for his help and advice on the Suez Rift, Sayeed and Gamal Gooda for field support, Rob Ellam for help with Sr-isotope analyses, and John McArthur for access to marine Sr-isotope look-up tables. James Jackson, Conrad Childs and Tom Blenkinsop are thanked for their constructive comments on the earlier version of the manuscript.

References

Ackermann, R.V., Schlische, R.W., Withjack, M.O., 2001. The geometrical and statistical evolution of normal fault systems: an experimental study of the effects of mechanical layer thickness on scaling laws. Journal of Structural Geology 23, 1803–1819.

Anders, M.H., Schlische, R.W., 1994. Overlapping faults, intrabasin highs and the growth of normal faults. Journal of Geology 102, 165–180.

Bentham, P.A., Westcott, W.A., Krebs, W.H., Lund, S.P., 1995. Magnetostratigraphic correlation and dating of the early to middle Miocene stratigraphy within the Suez Rift. American Association of Petroleum Geologists Bulletin 79, 1197–1198.

Cartwright, J.A., Trudgill, B.D., Mansfield, C., 1995. Fault growth by segment linkage: an explanation for scatter in maximum displacement and trace length data from the Canyonlands Grabens of SE Utah. Journal of Structural Geology 17, 1319–1326.

Contreras, J., Anders, M.H., Scholz, C.H., 2000. Growth of a normal fault system: observations from Lake Malawi basin of the east African rift. Journal of Structural Geology 22, 159–168.

Cowie, P.A., 1998. A healing–reloading feedback control on the growth rate of seismogenic faults. Journal of Structural Geology 20, 1075–1087.

Cowie, P.A., Gupta, S., Dawers, N.H., 2000. Implications of fault array evolution for syn rift depocentre development: insights from a numerical fault growth model. Basin Research 12, 241–262.

Dawers, N.H., Anders, M.H., 1995. Displacement–length scaling and fault linkage. Journal of Structural Geology 17, 607–614.

Dawers, N.H., Underhill, J.R., 2000. The role of fault interaction and linkage in controlling syn-rift stratigraphic sequences: Statfjord East area, northern North Sea. American Association of Petroleum Geologists Bulletin 84, 45–64.

Eliet, P.P., Gawthorpe, R.L., 1995. Drainage development and sediment supply within rifts, examples from the Sperchios basin, central Greece. Journal of the Geological Society of London 152, 883–893.

Garfunkel, Z., Bartov, Y., 1977. The tectonics of the Suez Rift. Geological Survey of Israel Bulletin 71, 1–41.

Gawthorpe, R.L., Leeder, M.R., 2000. Tectono-sedimentary evolution of active extensional basins. Basin Research 12, 195–218.

Gawthorpe, R.L., Fraser, A.J., Collier, R.E.Ll., 1994. Sequence stratigraphy in active extensional basins: implications for the interpretation of ancient basin fills. Marine and Petroleum Geology 11, 642–658.

Gawthorpe, R.L., Sharp, I.R., Underhill, J.R., Gupta, S., 1997. Linked sequence stratigraphic and structural evolution of propagating normal faults. Geology 25, 795–798.

Goldsworthy, M., Jackson, J., 2000. Active normal fault evolution in

Greece revealed by geomorphology and drainage patterns. Journal of the Geological Society of London 157, 967–981.

Gupta, S., Underhill, J.R., Sharp, I.R., Gawthorpe, R.L., 1999. Role of fault interactions in controlling synrift sediment dispersal patterns: Miocene, Abu Alaqa Group, Suez Rift, Egypt. Basin Research 11, 167–189.

Hardy, S., McClay, K.R., 1999. Kinematic modelling of extensional forced folding. Journal of Structural Geology 21, 695–702.

Jackson, C.A.-L., Gawthorpe, R.L., Sharp, I.R., 2002. Growth and linkage of the East Tanka fault zone, Suez rift: structural style and syn-rift stratigraphic response. Journal of the Geological Society of London 159, 175–187.

Krebs, W.N., Wescott, W.A., Nummedal, D., Gaafar, I., Azazi, G., Karamat, S., 1997. Graphic correlation and sequence stratigraphy of Neogene rocks in the Gulf of Suez. Bulletin Societie Geologie France 168, 63–71.

Leeder, M.R., Jackson, J.A., 1993. The interaction between normal faulting and drainage in active extensional basins, with examples from the western United States and central Greece. Basin Research 5, 79–102.

Leeder, M.R., Seger, M., Stark, C.P., 1991. Sedimentology and tectonic geomorphology adjacent to active and inactive normal faults in the Megara Basin and Alkyonides Gulf, Central Greece. Journal of the Geological Society of London 148, 331–343.

Mansfield, C., Cartwright, J., 2001. Fault growth by linkage: observations and implications from analogue models. Journal of Structural Geology 23, 745–763.

McArthur, J.M., Howarth, R.J., Bailey, T.R., 2001. Strontium isotope stratigraphy: LOWESS Version 3. Best-fit line to the marine Sr-isotope curve for 0 to 509 Ma and accompanying look-up table for deriving numerical age. Journal of Geology 109, 155–169.

Meyer, V., Nichol, A., Childs, C., Walsh, J.J., Watterson, J., 2002. Progressive localisation of strain during the evolution of a normal fault population. Journal of Structural Geology 24, 1215–1231.

Morley, C.K., 1999. Patterns of displacement along large normal faults: implications for basin evolution and fault propagation, based on examples from east Africa. American Association of Petroleum Geologists Bulletin 83, 613–634.

Morley, C.K., Vanhuwaert, P., De Batist, M., 2000. Evidence for high-frequency cyclic fault activity from high resolution seismic reflection survey, Rukwa Rift, Tanzania. Journal of the Geological Society of London 157, 983–994.

Moustafa, A.R., 1996. Internal structure and deformation of an accommodation zone in the northern part of the Suez rift. Journal of Structural Geology 18, 93–107.

Moustafa, A.R., Abdeen, A.R., 1992. Structural setting of the Hammam Faraun Block, eastern side of the Suez rift. Journal of the University of Kuwait (Science) 19, 291–310.

Moustafa, A.R., El Shaarawy, D.A., 1987. Tectonic setting of the northern Gulf of Suez. Proceedings of the 5th Annual Meeting of the Egyptian Geophysical Society, pp. 339–368.

Nicol, A., Walsh, J.J., Watterson, J., Underhill, J.R., 1997. Displacement rates on normal faults. Nature 390, 157–159.

Patton, T.L., Moustafa, A.R., Nelson, R.A., Abdine, S.A., 1994. Tectonic evolution and structural setting of the Suez Rift. In: Landon, S.M. (Ed.), Interior Rift Basins. American Association of Petroleum Geologists Memoir 59, pp. 7–55.

Prosser, S., 1993. Rift-related linked depositional systems and their seismic expression. In: Williams, G.D., Dobb, A. (Eds.), Tectonics and Seismic Sequence Stratigraphy. Geological Society Special Publication 71, pp. 35–66.

Richardson, M., Arthur, M.A., 1988. The Gulf of Suez–northern Red Sea Neogene rift: a quantitative basin analysis. Marine and Petroleum Geology 5, 247–270.

Roberts, S., Jackson, J., 1991. Active normal faulting in central Greece: an overview. In: Roberts, A.M., Yielding, G., Freeman, B. (Eds.), The Geometry of Normal Faults. Geological Society Special Publication 56, pp. 125–142.

Sharp, I.R., Gawthorpe, R.L., Underhill, J.R., Gupta, S., 2000a. Fault-propagation folding in extensional settings: examples of structural style and synrift sedimentary response from the Suez rift, Sinai, Egypt. Geological Society of America Bulletin 112, 1877–1899.

Sharp, I.R., Gawthorpe, R.L., Armstrong, B., Underhill, J.R., 2000b. Propagation history and passive rotation of mesoscale normal faults: implications for syn-rift stratigraphic development. Basin Research 12, 285–306.

Steckler, M.J., Berthelot, F., Lyberis, N., LePichon, X., 1988. Subsidence in the Gulf of Suez: implications for rifting and plate kinematics. Tectonophysics 153, 249–270.

Walsh, J.J., Watterson, J., 1988. Analysis of the relationship between displacement and dimensions of faults. Journal of Structural Geology 10, 239–247.

Young, M.J., Gawthorpe, R.L., Sharp, I.R., 2002. Architecture and evolution of syn-rift clastic depositional systems towards the tip of a major fault segment, Suez Rift, Egypt. Basin Research 14, 1–23.